

# Study of urban temperature profiles on the various land cover in the Jakarta Metropolitan Area, Indonesia

Hasti Widayasamratri<sup>1\*</sup>, Kazuyoshi Souma<sup>2</sup> and Tadashi Suetsugi<sup>3</sup>

Departement of Urban and Regional Planning, Sultan Agung Islamic University, Semarang, Indonesia

<sup>1,2,3</sup> University of Yamanashi, Japan.

Received: 2019-05-27  
Accepted: 2019-11-24

## Keywords:

urban thermal environment;  
urbanization;  
urban heat island;  
land cover

## Correspondent Email:

widya\_samratri@unissula.ac.id

**Abstract** This research aim to investigate the urban thermal environment profile and land cover classification in the Jakarta Metropolitan Area (JMA) in 1989 and 2013. Thermal environment conducted by installing fix point ground measurement of air temperature and land surface temperature. The land cover classification was carried out by using Landsat TM 5 and Landsat 7 ETM+ data sets. The diurnal variation of air temperature shows that Urban Heat Island (UHI) was occurring in urban and suburban JMA, which can be seen the slower cooling period in the urban area than suburban areas. Positive correlation between air temperature ( $T_a$ ) and land surface temperature ( $T_s$ ) on the brush ( $r^2 = 0.78$ ) and the asphalt surface ( $r^2 = 0.88$ ) is clearly shown during the study. The rapid urbanization was detected during 1989 to 2013 where the urban sprawl is spread over to the whole area of JMA. Urban built up is the dominant of high increase due to years, while vegetation is decreasing.

© 2019 by the authors. This article is an open access article distributed under the terms and conditions of the Creative Commons Attribution (CC BY NC) license <https://creativecommons.org/licenses/by-nc/4.0>

## 1. Introduction

Urbanization has various impacts on the urban environment. United Nation stated that during 1990 to 2015 the world's population had risen to 54%. For instance, 48% are Asian urban population, the most populated region in the world (United Nation, 2014). The rapid population in the urban area may expand rapidly within the past several decades where strongly affects the urban land features and suspected of urban temperature increases. The difference between thermal environment in urban areas and compare to rural surrounding areas named urban heat island (UHI) (Nastran et al, 2018; Debbage and Shepherd, 2015; Yin et al., 2018). The study of UHI related to land cover has been widely known in remote sensing study since it cover in wider area, low cost, and relatively fast (Rawat and Kumar, 2015; Hegazy and Kaloop, 2015).

There are three basic types of UHI, Canopy Layer Heat Island (CLHI), Boundary Layer Heat Island (BLHI) and Surface Urban Heat Island (SUHI). CLHI and BLHI are refers to atmospheric heating, and SUHI is temperature difference between urban and rural areas (Ali et al., 2017). Normally, UHI can be identified by using thermal infra red remote sensing satellite by extracting land surface temperature (LST) which generally use to assess urban green space, urban impervious surfaces, or land form configuration (Weng, 2012; Ali et al., 2017). Land cover is the physical features on earth surfaces that can be recognized by the distribution of vegetation, water, soil, and other manmade feature on the land as result of human activities (Rawat and Kumar, 2015).

Land cover is very close related to urbanization and urban surface temperature distribution which driven by anthropogenic and natural activities.

The used of remote sensing data satellite has been successfully proof to detect urbanization within land cover distribution (Edwin et al., 2015; Windusari et al., 2017) or urban thermal status (Van et al., 2015), however there are few researchers that explore connectivity of the observe LST temperature ( $T_s$ ) and air temperature ( $T_a$ ) before applied to the image data for further analysis. The urbanization impact to the urban thermal environment is quantify by measuring the urban thermal surfaces and the near surface atmosphere. The objective of this research are (1) to understand the relation of  $T_s$  and  $T_a$ , and (2) urban land cover profile in Jakarta Metropolitan Area (JMA) to reveal the urban thermal profile.

## 2. The Methods

The present Jakarta and its extended surrounding zone (Jakarta special region, Bogor, Tangerang, Bekasi) cover total 7500 km<sup>2</sup>, namely Jakarta Metropolitan Area (JMA) or Jabodetabek (Jakarta, Bogor, Depok, Tangerang, and Bekasi). JMA covered 0.33% of the Indonesia land area where 12% of Indonesia's total population are living. Due to 2010s, the built-up of Jakarta has been successfully growth to be a mega city and sprawls to its peripheries crosses provinces of Greater Jakarta, West Java, and Banten (World Bank, 2015). Figure 1 shows the study area at JMA where has been spread as a mega city.

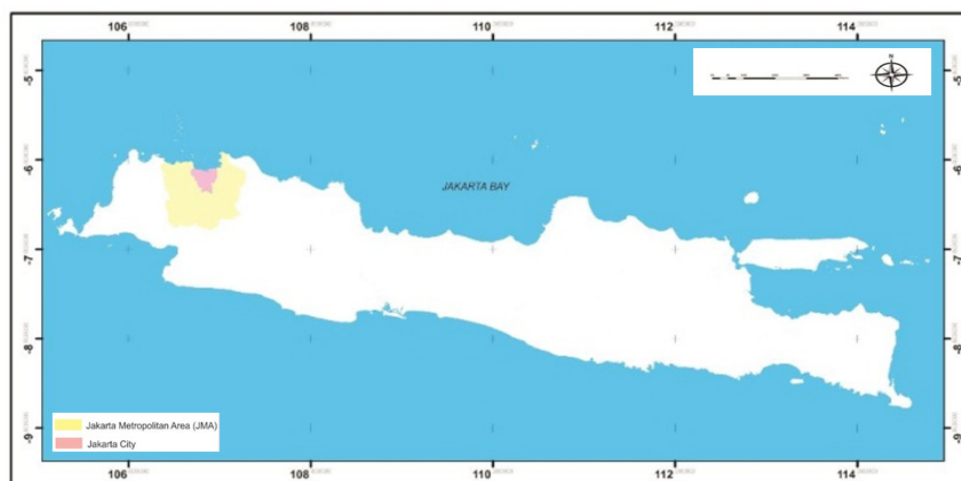


Figure 1. Jakarta Metropolitan Area, Indonesia.

### Urban thermal observations in Jakarta Metropolitan Area (JMA)

The Fix point measurement was conducted to investigate and validate the thermal environment profile in JMA. There were two types temperature measurement during the observation period, ground measurement of  $T_a$  and  $T_s$ , both are conducted in 20 September– 15 October 2013 for 24 hours to observe the diurnal variation of air and surface temperature. We installed five thermal equipments in the pointed areas to observe the diurnal  $T_a$  and  $T_s$ .  $T_a$  is an energy exchange of heat volume where flowing into radiation, conduction, and convection in the near surface atmosphere. By the time,  $T_s$  is governed from solar radiation, conduction, and turbulence fluxes. In surface energy balance terminology  $T_s$  generated by sensible heat flux density ( $Q_H$ ) from the earth surfaces to the atmosphere and turn back to the earth ( $Q_G$ ) (Oke et al., 2017). To understand the relation of the earth surfaces heat to the near surface atmosphere, we choose brush and asphalt. Brush is correspond to the dry and bare soil, whereas asphalt is correspond to the urban or built-up environment.

### Land cover classification

To classify and identify the land cover change in the period we choose Landsat TM 5 in 1989 and Landsat ETM+ in 2006 as a base of 2013's land cover latest information. The 1989's imagery was represented JMA's land cover in early 1990. The 2013's land cover information was conducted by update 2006's imagery since we could not find the ideal satellite imagery data set to classify. To execute the land cover classification process, the supervised classification technique is chosen.

There are three steps to proceed supervise classification in remote sensing image, (1) identifies representative training area for each land cover type, (2) categorize each pixel into land cover class, (3)

digitalize the result as a thematic map. The investigation of this study, mostly was done in September-October of meteorological data time series (1990-2013) as the peak time of the dry season in Indonesia. A ground survey was done in order to proceed the land cover accuracy by collected 20 points for each land cover categories. The targeted categories are : (1) vegetation, (2) water body, (3) brush, (4) urban/built-up. A high spatial resolution of image satellite was chosen to evaluate the land cover in 1989, and a direct field survey was done to evaluate the land cover in 2006. A kappa coefficient and overall accuracy was used to measure the classification accuracy (Hua and Ping, 2018).

## 3. Result and Discussion

### Urban thermal profile in Jakarta

We observed the 24 hour diurnal  $T_a$  in 1.5 m height measurement tools in four locations, Bogor, Depok (the equipment broken) Kramatjati (Jakarta core city), Tangerang, and Bekasi. Figure 2 shows the fix point measurement of diurnal  $T_a$ . The investigation started at the midnight when most atmospheric process and wind speed are getting decrease according to the meteorological data. We can see the graph, at the midnight to before sunrise (0:00 – 05:00 local time), the  $T_a$  was gradually decreased. Although whole cities of  $T_a$  to be decreasing, Bogor, the southern part of JME has the lowest (23.5°C) because was getting less influence of the sea breeze from the Java sea (northern Jakarta), whereas Tangerang, the most southern part was getting more influence of the sea breeze where impacted to the heat loss. In the daytime, the temperature reached the peak level and cooling down in around 15 p.m. Here, Jakarta (urban) were kept on their higher temperature than Bogor (suburban). Urban area much slower in cooling and has stronger heat than the suburban area at the night time, this can be identified as the urban heat island (UHI) phenomenon.

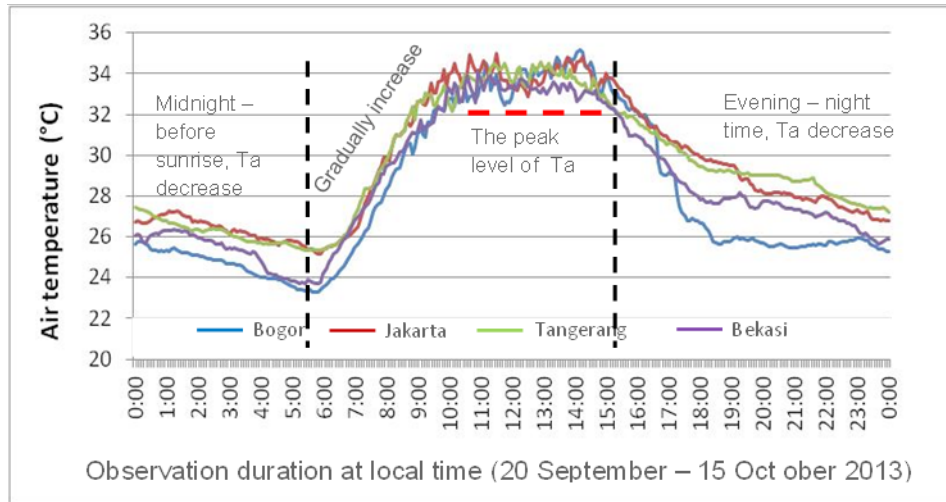


Figure 2. Diurnal Ta in Jakarta Metropolitan Area, Indonesia.

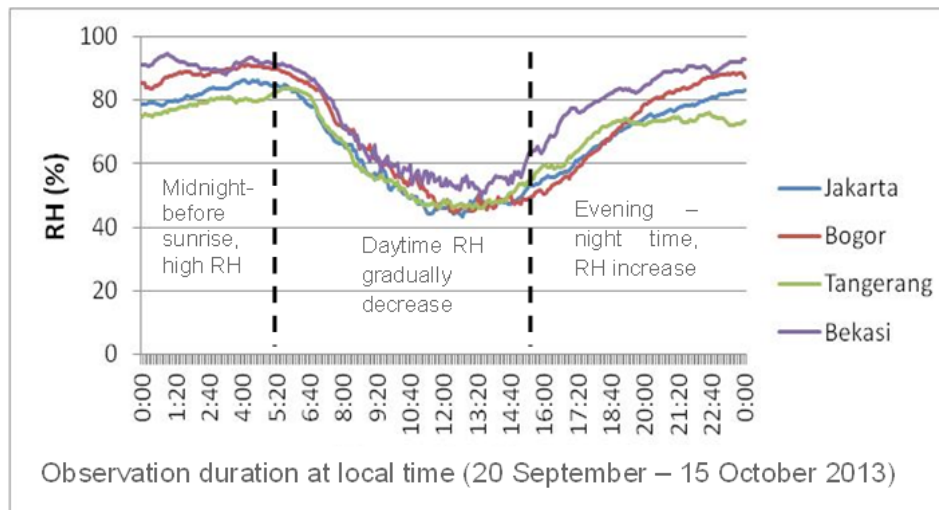


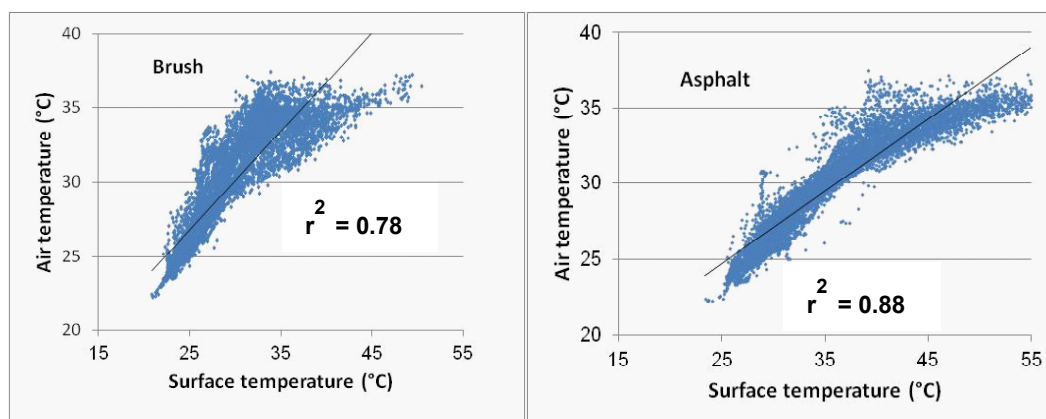
Figure 3. Diurnal RH in Jakarta Metropolitan Area.

Figure 3 shows the diurnal relative humidity in observation field. Lower relative humidity (RH) was occurring during the night time to early morning in the high urbanized area caused by the low vegetation evapotranspiration. In the daytime, the relative humidity in the whole area was decreasing caused by the high intensity of solar radiation and the sea breeze (Java sea) which carried water vapor is penetrated to the urban center. In the early evening to the midnight RH was generally increased because the solar radiation and the sea breeze is become weak, but in some specific area which sited in the coastal area (Tangerang and Bekasi) it seems to be higher than the others. At the midnight time, RH was high in the suburbs (Bogor) caused by the mountain breeze which carried water vapor was penetrate this area.

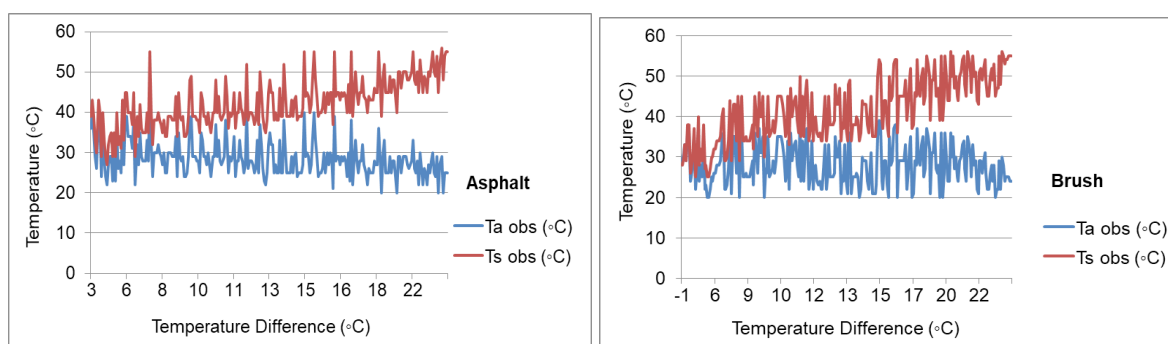
Previously, we investigated the diurnal Ta and RH (Figure 2 and Figure 3) of thermal profile in JMA.

To connect the LST imagery in order to estimate Ta in the urban form, we should understand the relationship of both by applying a statistical technique to the represent types of land cover. In this study, we choose asphalt which corresponds to the urban or built-up area and brush because both are the dominant urban impervious surface in JMA. The statistical technique based on Pearson's correlation was done to analyze the finding. The t statistic (t), and the regression (r) are calculated for the samples. The correlation coefficient between Ta and Ts is represented in r, where r values close to 1 represent a high positive correlation and r values close to -1 represent a high negative correlation (Rosnow et al., 2000; Hathway and Sharples, 2012). The temperature difference between the Ta and Ts are calculated using :

$$\Delta T = T_s \text{ observation} - T_a \text{ observation} \quad (1)$$

Figure 4. Scatter plot of  $T_s - T_a$  in (a) brush and (b) asphalt.Table 1. Mean  $\Delta T$ , correlation ( $r$ ),  $t$  statistic ( $t$ ), minimum and maximum for the brush and asphalt temperature.

	Mean $\Delta T$	$r^2$	$t$	SE	Min temp ( $^{\circ}\text{C}$ )	Max temp ( $^{\circ}\text{C}$ )
Brush	13.76	0.78	-37.1	0.4	-1	31
Asphalt	13.53	0.88	-34	0.3	3	30

\* $p < 0.05$ Figure 5. Value of temperature difference of  $T_s - T_a$  in brush and asphalt surfaces.

The  $r$  values of  $T_s - T_a$  in brush and asphalt shown a high positive correlation and statistically significant ( $r^2_{\text{brush}} = 0.78$ ,  $t\text{-stat} = -37.1$ ,  $p < 0.05$ ;  $r^2_{\text{asphalt}} = 0.88$ ,  $t\text{-stat} = -34$ ,  $p < 0.05$ ) in representing point observation (Figure 4) which mean,  $T_s$  and  $T_a$  values has very close correlation of thermal situation (Table 1).

Figure 5 shows the temperature difference of  $T_s - T_a$  in brush and asphalt surfaces. The minimum value of temperature difference of brush surface is  $-1^{\circ}\text{C}$  and maximum value of temperature difference is  $31^{\circ}\text{C}$ . On asphalt surface, the minimum value of temperature difference is  $3^{\circ}\text{C}$  and the maximum value of temperature difference is  $30^{\circ}\text{C}$  (Table 1). In both surface types,  $T_s$  has higher temperature value than  $T_a$  with mean difference of temperature is  $13.76^{\circ}\text{C}$  on brush surface and  $13.53^{\circ}\text{C}$  on asphalt surface.  $T_s$  is pay significance contribution in the climate change impacts simulation on the environment, and ecology since both has different factors in the energy exchange

process (Luo et al., 2018). Commonly, the temperature difference on  $T_s - T_a$  is followed by hourly incident of solar radiation (Springs et al., 2011).

### JMA land cover distribution as an urbanization impact

Land cover extraction from satellite remote sensing data given critical role in providing large coverage spatial information, as well as the thermal information at the time satellite overpass. We were classified and mapped the spatial distribution of JMA land cover by using Landsat time series data which downloaded from <http://glcf.umd.edu/data/>. Land cover maps were governed using supervised classification based on the Maximum Likelihood algorithm in Multispec software. Land cover types were classified including vegetation, urban/built-up, brush, and water body (Figure 6).

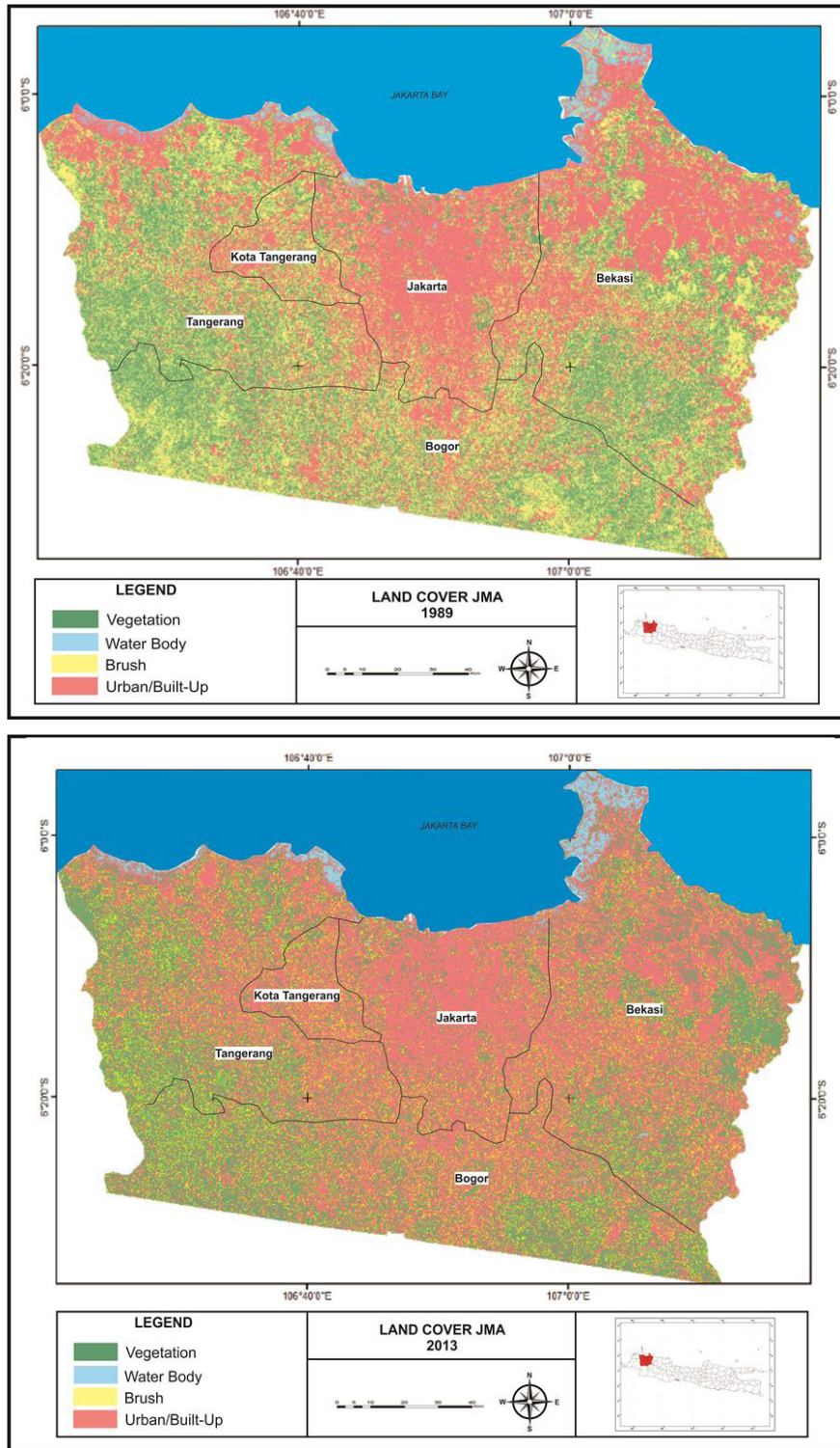


Figure 6. JMA land cover distribution in 1989 (above) and 2013 (below).

Accuracy assessment of the land use classification results obtained showed an overall accuracy of 85.9% in 1989 and 93.5% in 2013. The Kappa coefficients for both maps were 0.75 and 0.83 respectively. During 1989 and 2013 there were some significant change of land cover. In 1989 land cover classification, urban/built-up area 35.42% (1,692 km<sup>2</sup>), vegetation 32.16% (1,536 km<sup>2</sup>), brush 30.62% (1,463 km<sup>2</sup>), water body 1.7% (85

km<sup>2</sup>). In 2013, urban/built-up area 70.5% (3,369 km<sup>2</sup>), vegetation 14.2% (676 km<sup>2</sup>), brush 13.5% (646 km<sup>2</sup>), water body 1.8% (85 km<sup>2</sup>) (Table 2). Based on the land cover distribution, the urban/built-up area increased up to 35%, brush was decreased up to 17.1% and vegetation was decreased up to 18%. This study was emphasized in the degree of land use changing, and did not investigate the type of land cover conversion.

Table 2. Land cover distribution in JMA.

Land cover	Land cover distribution in JMA					Change (sq. km)
	1989		2013			
	Area (sq. km)	%	Area (sq. km)	%		
Brush	1,463	31	646	14		-817
Vegetation	1,536	32	676	14		-860
Urban/Built-up	1,692	35	3,369	71		1,677
Water body	85	2	85	2		0
Total	4,776		4,776			

#### 4. Conclusion

Urbanization is the key of land use/land cover change that impacted to the surface thermal environment. We carried out the ground point air temperature and land surface temperature measurements in order to understand the connectivity of both types of thermal situation in urban surfaces. Furthermore, to observe the land cover in JMA, we used two different years of satellite image data sets. The types of land cover are contributing to the surface temperature and indicate the urbanization distribution.

The diurnal variation of air temperature was starting to increase in 6 a.m. and had the peak in around 15 p.m. on all the observation points (Jakarta/Kramatjati, Bogor, Tangerang, Bekasi). An UHI was detected in the JMA area since there is a different air temperature cooling period between urban (Jakarta/Kramatjati, Tangerang, and Bekasi) and suburban (Bogor). The urban areas had slower cooling periods than suburban. The study also shows that there are positive correlation between air temperature and surface temperature in the earth surfaces where detected to the asphalt and brush surfaces by using an infrared thermometer. This evidence shows, that the 1.5 m air temperature is highly influenced by the heat energy of earth surface features, both artificial or natural surfaces.

This research shows that urbanization in JMA was amazingly detected using satellite imagery datasets. In 1989 the urbanization was only concentrated in the middle part, but in 2013 the urbanization has been spread over to the whole area and seems to be moved to the southern part. The dominant increase of land cover change is in urban built up, whereas the decrease is on vegetation surface. The micro thermal details of the observation on individual ground measurement and compare to the land cover change, there is clearly understood that land use/land cover change impacts to the thermal environment of the earth surfaces. Urban sprawl has significant influence on heat intensity where might be has contributed to the climate change. A further measurement and analysis of urban thermal environment should be done by using this research result to improve the latest issue of urbanization effects in JMA.

#### Acknowledgement

The author would like to thank the ICRE (Interdisciplinary Centre for River Basin Environment), University of Yamanashi, Japan, for supporting this study.

#### References

- Ali, S. B., Patnaik, S., & Madguni, O. (2017). Microclimate land surface temperatures across urban land use/ land cover forms. *Global J. Environ. Sci. Manage*, 3(3), 231–242. <https://doi.org/10.22034/gjesm.2017.03.03.001>
- Debbage, N., & Shepherd, J. M. (2015). The urban heat island effect and city contiguity. *Computers, Environment and Urban Systems*, 54, 181–194. <https://doi.org/10.1016/j.compenvurbsys.2015.08.002>
- Edwin, E., Saidi, A., Aprisal, A., Yulnafatmawita, Y., & Carolita, I. (2015). Spatial and Temporal Analysis of Land Use Change for 11 years (2004–2014) in Sub-Watershed Sumpur Singkarak. *International Journal on Advanced Science, Engineering and Information Technology*, 5(5), 326–329. Retrieved from [http://ijaseit.insightsociety.org/index.php?option=com\\_content&view=article&id=9&Itemid=1&article\\_id=563](http://ijaseit.insightsociety.org/index.php?option=com_content&view=article&id=9&Itemid=1&article_id=563)
- Hathway, E. A., & Sharples, S. (2012). The interaction of rivers and urban form in mitigating the Urban Heat Island effect : A UK case study. *Building and Environment*, 58, 14–22. <https://doi.org/10.1016/j.buildenv.2012.06.013>
- Hegazy, I. R., & Kaloop, M. R. (2015). Monitoring urban growth and land use change detection with GIS and remote sensing techniques in Daqahlia governorate Egypt. *International Journal of Sustainable Built Environment*, 4(1), 117–124. <https://doi.org/10.1016/j.ijsbe.2015.02.005>
- Hua, A. K., & Ping, O. W. (2018). The influence of land-use/ land-cover changes on land surface temperature: a case study of Kuala Lumpur metropolitan city. *European Journal of Remote Sensing*, 51(1), 1049–1069. <https://doi.org/10.1080/22797254.2018.1542976>
- Luo, D., Jin, H., Marchenko, S. S., & Romanovsky, V. E. (2018). Geoderma Difference between near-surface air, land surface and ground surface temperatures and their influences on the frozen ground on the Qinghai-Tibet Plateau. *Geoderma*, 312(September 2017), 74–85. <https://doi.org/10.1016/j.geoderma.2017.09.037>
- Nastran, M., Kobal, M., & Eler, K. (2018). Urban heat islands in relation to green land use in European cities. *Urban Forestry and Urban Greening*, (December 2017), 1–9.

- <https://doi.org/10.1016/j.ufug.2018.01.008>
- Nastran, M., Kobal, M., & Eler, K. (2019). Urban heat islands in relation to green land use in European cities. *Urban Forestry and Urban Greening*, 37(January 2018), 33–41. <https://doi.org/10.1016/j.ufug.2018.01.008>
- Oke, R. T.; Mills, G.; Christen, A.; Voogt, A. J. (2017). *Urban Climates* (1st ed.). University of Cambridge: Cambridge University Press. <https://doi.org/10.1017/9781139016476>
- Rawat, J. S., & Kumar, M. (2015). Monitoring land use/cover change using remote sensing and GIS techniques: A case study of Hawalbagh block, district Almora, Uttarakhand, India. *Egyptian Journal of Remote Sensing and Space Science*, 18(1), 77–84. <https://doi.org/10.1016/j.ejrs.2015.02.002>
- Rosnow, R. L.; Rosenthal, R. and Rubin, D.B. (2000). Contrasts and Correlations in Effect-size Estimation Contrast and Effect - Size Estimation. *Psychological Science*, 11(6), 446–453. <https://doi.org/10.1037/1096-3445.11.6.446>
- Springs, C., Collins, F., Chase, C., & Springs, C. (2011). Evaluation of the Relationship between Air and Land Surface Temperature under Clear and Cloudy Sky Conditions. *Journal of Applied Meteorology and Climatology*, 50, 767–775. <https://doi.org/10.1175/2010JAMC2460.1>
- United Nation, Department of Economic and Social Affairs, P. D. (2014). *World Urbanization Prospects: The 2014 Revision, Highlights (ST/ESA/SER. A/352)*. United Nation.
- Van, T. T., Duong, H., & Bao, X. (2015). Characteristics of Urban Thermal Environment from Satellite Remote Sensing Data in Ho Chi Minh City, Vietnam. *Conference Proceedings Paper – Remote Sensing Characteristics*, 1–7.
- Weng, Q. (2012). Remote sensing of impervious surfaces in the urban areas: Requirements, methods, and trends. *Remote Sensing of Environment*, 117, 34–49. <https://doi.org/10.1016/j.rse.2011.02.030>
- Windusari, Y., Hanum, L., & Lestari, M. S. (2017). Analysis and Identification of Landuse on the Coastal Environment of South Sumatra using GIS. *International Journal on Advance Science Engineering Information Technology*, 7(3), 785–791.
- World Bank. (2015). *East Asia's Changing Urban Landscape: Measuring a Decade of Spatial Growth. Urban Development Series*. Washington, DC: World Bank. <https://doi.org/10.1596/978-1-4648-0363-5>.
- Yin, C., Yuan, M., Lu, Y., Huang, Y., & Liu, Y. (2018). Effects of urban form on the urban heat island effect based on spatial regression model. *Science of the Total Environment*, 634, 696–704. <https://doi.org/10.1016/j.scitotenv.2018.03.350>